Experimental evaluation of the dowel-bearing strength of laminated flattened-bamboo lumber perpendicular to grain

Haitao Li[a, b*], Yue Chen[a, b], Dong Yang[a, b], Rodolfo Lorenzo[c], Conggan Yuan[d]

[a] College of Civil Engineering, Nanjing Forestry University, Nanjing 210037, China;

[b] Joint International Research Laboratory for Bio-composite Building Materials and Structures, Nanjing Forestry University, Nanjing 210037, China；

[c] University College London, London WC1E 6BT, UK;

[d] Jiangxi Feiyu Bamboo Materials Holding Co., LTD., Yichun 330700, China.

*Corresponding author: Haitao LI, Professor, E-mail: lhaitao1982@126.com

Abstract: This paper examines the dowel-bearing strength of laminated flattened-bamboo lumber (LFBL) perpendicular to grain under the influence of the flattened-bamboo arrangement method, the bolt diameter, and specimen size in accordance with ASTM D5764-97a. There were 360 specimens tested in total. As a result of the test results, it was demonstrated that the arrangement method of flattened bamboo panels significantly

Abbreviations:

1. LFBL: laminated flattened-bamboo lumber
2. The groups "RT", "TR", "RL", and "TL" are related to the load directions and the direction of the bolts, and the details are given in the text.
3. LBL: laminated bamboo lumber
4. PBSL: parallel bamboo strand lumber
5. LLW :larch laminated wood
6. GB: glulam bamboo
7. THW: tropical hard wood
8. GLGB: glued laminated Guadua bamboo

affected the dowel-bearing strength of the LFBL. In two of the groups (bolt direction perpendicular to the grain), the dowel-bearing strength was significantly greater than in the other two groups (bolt direction parallel to the grain). According to the arrangement method of the bamboo panels, the size effect on dowel-bearing strength varies. However, the dowel-bearing strength always decreased as the diameter of the bolt increased. Four typical failure modes and load-displacement curves were classified. Results of the tests were compared with those calculated by predicting formulas from other studies, allowing empirical equations for predicting the dowel-bearing strength of LFBL specimens to be developed.

Key words: composite materials; compression; laminated; testing

1 Introduction

The construction industry has always had a significant impact on the environment. It is in the interest of countries to promote research on new, environmentally friendly building materials, such as bamboo [1] and wood [4], in order to change the mode of development at the expense of consuming resources and polluting the environment [7]. Due to its excellent mechanical properties, light weight, and short growth cycle, bamboo is considered a good alternative to wood for construction [8]. A bamboo or wood structure is constructed by connecting its components, and the performance of the connections directly impacts the structure's strength, safety, applicability, and durability. A bolted joint is commonly used in structures due to its simplicity, dependability, and convenience, which enables the mechanical properties of the materials to be fully utilized [11]. Bolted joints fail primarily due to bolt bending failure and bamboo or timber bearing failure [13], so calculating the bearing capacity of bolted connections requires a measurement of the dowel-bearing strength of bamboo or wood.

To address the geometric and mechanical variability of natural bamboo poles, the technology of engineered bamboo was developed. Laminated bamboo lumber (LBL) is one of the engineered bamboo products [15], and due to its excellent physical and mechanical properties [16], it can meet the needs of multi-story structures. Nonetheless, the use of bamboo in the production of traditional LBL was typically less than 50% [17]. To increase the utilization rate of bamboo, researchers have studied bamboo flattening technology since the 1980s [18], which involves softening the bamboo at a high temperature, flattening it, and then drying it [19]. After decades of research, Li et al. [21] proposed a non-cracking method for bamboo flattening. This new method can increase the utilization rate of bamboo by 20%, reduce the amount of adhesive used during the production process by 30%, and increase the value of bamboo products by over 25%. Using the bamboo panels produced by this new technology and combining them with the traditional method of producing LBL, a new type of engineered bamboo laminated flattened-bamboo lumber (LFBL) was manufactured.

Numerous studies have been conducted on the dowel-bearing capacity of wood and wood products, whereas the majority of research on engineered bam The American standard ASTM D5764 [22] and the European standard BS EN 383 [23] were primarily cited in the test method for measuring the dowel-bearing strength of wood. Santos et al. [24] compared the dowel-bearing capacity of maritime pine wood tested in accordance with ASTM D5764 and BS EN 383. The full-hole test method recommended by BS EN 383 was found to be more susceptible to bolt bending than the half-hole test method recommended by ASTM D5764. In contrast, for laminated veneer bamboo (LVB) [25] both Finite Element Analysis (FEA) and experimental analysis revealed that the shear stress within the half-hole specimen became the primary cause of failure, and that the full-hole test method was more representative of actual connection conditions. In the review by Ottenhaus et al. [26], for hardwoods and engineered wood products with an embedment strength greater than the dowel yield moment, the half-hole test is recommended; otherwise, the full-hole test is recommended.

Researchers also concluded that the tested dowel-bearing strength varies with temperature, bolt diameter, moisture content, sample size, and loading direction. Cui et al. [27] tested the dowel-bearing strength of wood at temperatures ranging from 0 °C to 250 °C, and the results indicated that the dowel-bearing strength of wood decreased as the temperature increased. It can be concluded that high temperatures and fire have a detrimental effect on the performance of joints in wood structures. Researchers have not reached a consistent conclusion regarding the impact of bolt diameter and specimen size on the dowel-bearing performance of wood. The research conducted by Rammer [28] revealed that the diameter of the bolt had no effect on the dowel-bearing strength of hard wood, whereas the initial stiffness varied with different bolt diameters. Sawata and Yasumura [29] reached the same conclusion based on their study of the dowel-bearing strength of parallel-grain wood. In Li [11], Whale and Smith's study [30], however, the dowel-bearing strength of PBSL and wood decreased as the bolt diameter increased. Cui et al. [31] tested the dowel-bearing strength of LBL using the full-hole method and discovered that the dowel-bearing strength remained constant with the change of specimen width but decreased significantly with the increase of specimen thickness and length. Nevertheless, Li [11] believed that the size would not affect the dowel-bearing strength as long as the specimen met the minimum size requirements.

In conclusion, the effect of various factors on the dowel-bearing strength of wood and engineered bamboo is distinct. In this paper, the dowel-bearing strength of LFBL perpendicular to grain was investigated using the half-hole test under the influence of the flattened-bamboo panels, bolt diameter, and specimen size. To verify the dependability of LFBL, its dowel-bearing strength was compared to that of other timber-and-bamboo-based products. The applicability of the existing calculation theory to the dowel-bearing strength of LFBL was evaluated by comparing and analyzing the dowel-bearing strength predicted by different standards and equations in the literature.

2 Test design

2.1 Materials

The raw bamboo was *phyllostachys pubescens* harvest from Jiangxi, China, at the age of 3-5 years, and was produced into flattened bamboo by the new non-crack bamboo flattening method. The size of flatted bamboo panel was 70 mm or 100 mm in width, 1000 mm in length and 5 mm in thickness. Then the panels were produced into LFBL according to the two-step manufacturing process of traditional LBL. First the panels were made into flattened bamboo board with the width from 600 mm to 700 mm under the positive pressure of 12 MPa, size pressure of 4 MPa, and temperature of 95℃ for 2.5 minutes. Then the boards were stacked 20 layers and compressed under the pressure of 18 MPa, temperature of 95℃ for 2 hours. All the bamboo products for tests were processed by Jiangxi Feiyu Bamboo Materials Holding Co., LTD. Fig. 1 shows the processing steps of LFBL and the product photos taken on site. The adhesive was urea-formaldehyde resin produced by Dynea, Lillestrøm, Norway. The mechanical properties of the material were tested in accordance with ASTM D143-2014 [32] (20 repetitions of each treatment), and all specimens were weighed and measured to obtain the mean density and moisture content. The results are shown in Table 1.

Table 1 The mechanical properties of LFBL

	compression			tension			Density/kg/m^3	Moisture content
	R	T	L	R	T	L		
strength/MPa	43.1	19.0	56.2	1.8	4.3	106.9	743	8.5%
E/MPa	580.9	1124.5	9631.2	1459.6	5112.5	10151.1		

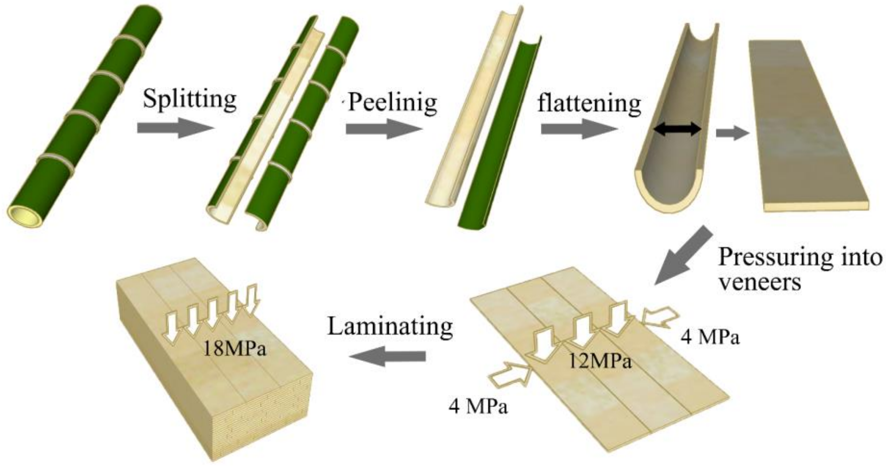

(a) The schematic of processing steps

(b) The Row bamboo

(c) The flattened-bamboo panels

(d) The flattened-bamboo veneers

(e) Pressing

(f) Drilling

Fig. 1. The processing of LFBL

2.2 Test method

The half-hole test method (Fig. 2 (e)) was utilized in accordance with ASTM D5764 [22]. In beam-column bolted connections, the dowel hole in the beam section is typically loaded in compression perpendicular to the grain; however, the arrangement of flattened-bamboo panels is variable. In various instances, the specimens were therefore classified into four categories. As shown in Fig. 2 (a-d), they were RT, TR, RL, and TL groups.

Cross-sections of vascular bundles are depicted in the figure, and "L" indicates the direction of fiber growth. Take the RT group as an example: the first letter "R" indicates that the load direction is parallel to the radial direction of the LFBL, while the second letter "T" indicates the direction of the bolts. Further, in order to examine the effect of specimen size and bolt diameter, the parameters of the RT and TR groups' specimens were altered, as dowel connections in these two pressure states (bolt direction is perpendicular to the fibers) are more commonly used in practical applications. The parameter levels were set as follows: length (*L*) and width (*W*): 60 mm, 70 mm, 80 mm, 90 mm, 100 mm, thickness (*T*): 30 mm, 35 mm, 40 mm, 45 mm, 50 mm, bolt diameter (*D*): 12 mm, 14 mm, 16 mm, 18 mm, 20 mm. he final rule for group names was as follows: A third letter 'S' indicates that the dimensions of this group of specimens fully comply with ASTM D5764; otherwise, it indicates an influence factor. "RTD12" is an example; the letter D indicates that only the bolt diameter was different from the RTS group, which was 12 mm. Table 2 presents the design specifications.

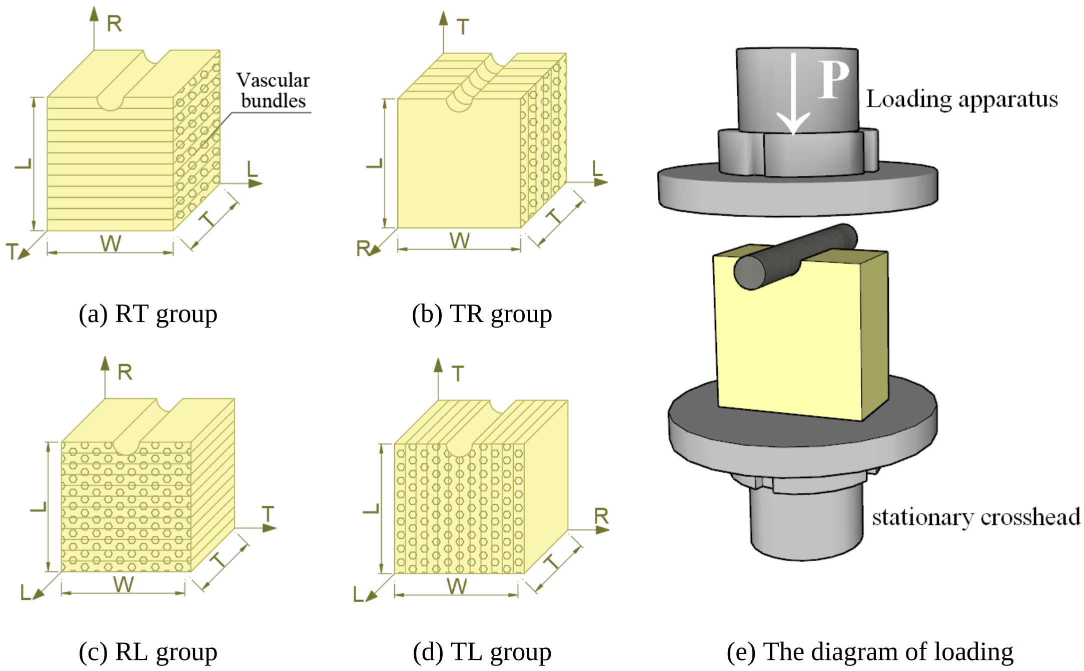

(a) RT group (b) TR group

(c) RL group (d) TL group (e) The diagram of loading

Fig. 2. Specimen categories and loading process

Table 2 The design of specimens

Groups	D/mm	L/mm	W/mm	T/mm	Groups	D/mm	L/mm	W/mm	T/mm

RLS	16	80	80	40	TLS	16	80	80	40
RTS	16	80	80	40	TRS	16	80	80	40
RTD12	12	80	80	40	TRD12	12	80	80	40
RTD14	14	80	80	40	TRD14	14	80	80	40
RTD18	18	80	80	40	TRD18	18	80	80	40
RTD20	20	80	80	40	TRD20	20	80	80	40
RTL60	16	60	80	40	TRL60	16	60	80	40
RTL70	16	70	80	40	TRL70	16	70	80	40
RTL90	16	90	80	40	TRL90	16	90	80	40
RTL100	16	100	80	40	TRL100	16	100	80	40
RTW60	16	80	60	40	TRW60	16	80	60	40
RTW70	16	80	70	40	TRW70	16	80	70	40
RTW90	16	80	90	40	TRW90	16	80	90	40
RTW100	16	80	100	40	TRW100	16	80	100	40
RTT30	16	80	80	30	TRT30	16	80	80	30
RTT35	16	80	80	35	TRT35	16	80	80	35
RTT45	16	80	80	45	TRT45	16	80	80	45
RTT50	16	80	80	50	TRT50	16	80	80	50

In the structural laboratory of Nanjing Forestry University, all of the tests were conducted using a 50 kN-capacity electro-hydraulic servo universal testing machine（Fig. 3 (a)）. The displacement-control load method was adopted during all the tests at a rate of 1.5 mm/min, and each set of tests was repeated 10 times. The dowel-bearing strength of LFBL was calculated by Eq. (1) based on 5%-diameter off-set method recommended by ASTM D5764 (Fig. 3 (b)).

$$f_{\mathrm{e,y}} = P_{\mathrm{y}} / DT \tag{1}$$

Where, $f_{\mathrm{e,y}}$ is the 5%-diameter off-set dowel-bearing strength, P_{y} is the yield load obtained by the 5%-diameter off-set method, D is the bolt diameter, T is the thickness of specimen.

(a) Testing site

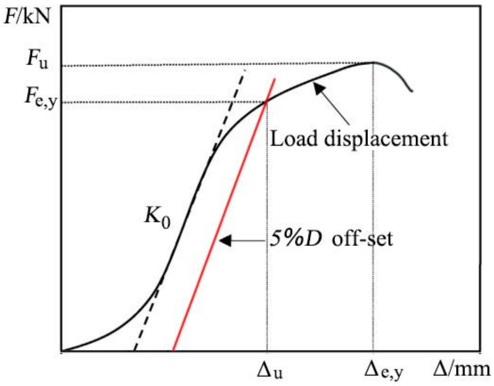

(b) 5% diameter off-set method

Fig. 3. Test method and device

3 Test results and analysis

The results of the tests are shown in Table 3. The dowel-bearing strength of LFBL ranged from 19.8 MPa to 35.3 MPa during testing., and the greatest coefficient of variation (COV) among all groups was 12.4%. The initial stiffness of the specimens ranged from 6.1 kN/mm to 14.1 kN/mm with a COV less than 15.3%. The ratio of ultimate dowel-bearing strength (f_u) to 5% D dowel-bearing strength ($f_{e,y}$) was greater than 1.5 for all specimens in the RT and TR groups, but it was less than 1.5 for specimens in the RL and TL groups. After reaching the yield load, the dowel-bearing capacity of the RT and TR groups of specimens had considerable room to increase.

Table 3 Test results

Groups	$f_{e,y}$ /MPa	COV /%	k_0 /kN/mm	COV /%	f_u /MPa	COV /%	$f_u/f_{e,y}$
RLS	19.8	6.4	6.6	9.3	27.3	4.2	1.4
TLS	20.2	10.4	9.8	13.4	20.8	13.4	1.0
RTS	26.8	5.5	8.7	12.4	48.7	5.3	1.8
RTD12	29.0	8.7	8.4	10.6	51.8	10.8	1.8
RTD14	27.9	9.5	8.5	11.1	50.3	7.6	1.8
RTD18	26.5	12.1	9.6	14.0	47.8	19.1	1.9
RTD20	26.0	6.0	10.3	9.4	44.7	12.3	1.7
RTL60	27.7	9.6	9.8	13.0	48.2	11.3	1.7
RTL70	26.5	5.7	9.2	7.8	45.5	5.3	1.7

RTL90	26.6	3.9	9.1	4.7	42.1	6.4	1.6
RTL100	26.1	8.4	7.5	12.7	44.3	11.7	1.7
RTW60	22.0	4.3	8.2	14.5	45.9	5.3	2.1
RTW70	24.6	7.9	8.8	11.6	48.9	11.8	2.0
RTW90	27.1	3.0	9.2	13.4	46.0	6.2	1.7
RTW100	27.3	9.2	8.4	15.3	43.8	7.3	1.6
RTT30	25.6	3.5	6.1	6.5	43.5	7.0	1.7
RTT35	25.6	6.8	8.2	5.9	45.5	8.7	1.8
RTT45	26.6	3.6	9.5	7.0	45.3	4.7	1.7
RTT50	25.8	2.2	10.8	4.0	42.5	9.4	1.6
TRS	32.0	9.4	11.8	9.4	50.8	10.9	1.6
TRD12	34.5	8.6	11.3	11.5	54.3	10.8	1.5
TRD14	32.9	7.0	11.9	5.6	51.9	8.6	1.6
TRD18	31.0	12.4	12.6	9.7	50.6	12.1	1.7
TRD20	30.9	7.6	14.1	8.4	51.2	7.8	1.7
TRL60	31.9	7.9	12.5	10.1	52.4	8.8	1.7
TRL70	32.0	1.9	11.9	3.1	50.8	2.6	1.6
TRL90	33.1	7.8	10.9	9.3	51.4	7.4	1.6
TRL100	32.9	2.2	10.9	2.7	53.1	6.7	1.6
TRW60	34.3	9.1	11.5	6.8	58.7	9.3	1.7
TRW70	33.7	3.2	11.2	10.9	56.7	5.2	1.7
TRW90	31.9	9.4	11.6	6.1	48.7	10.7	1.5
TRW100	33.2	4.7	11.7	6.1	49.7	4.8	1.5
TRT30	30.2	2.4	7.6	4.4	47.2	5.8	1.5
TRT35	30.8	3.0	10.0	5.1	50.4	5.5	1.6
TRT45	34.2	9.8	13.3	9.3	53.6	11.4	1.6
TRT50	35.3	4.3	13.7	5.3	54.4	5.2	1.5

3.1 Analysis of failure phenomena

The failure modes of all specimens can be classified into 4 categories.

3.1.1 Failure mode I

RT specimens exhibited Interlaminar fracture caused by incongruous deformation between the compression area and the specimen's exterior, as shown in Fig. 4 （a, b）. The semicircular hole of the specimen shrank and deformed toward the center as the load increased, while the upper end, left, and right sides of the specimen did not belong to the pressure area and exhibited minimal deformation. Thus, the deformation was inconsistent, resulting in the interlaminar fracture at the edge of the specimen. In the case of a small diameter and a wide width, the cracks were few and microscopic (Fig. 4 (a)), whereas in the case of a small diameter and a narrow width, the cracks were numerous and wider (Fig. 4 (b)).

3.1.3 Failure mode II

The failure mode II was tearing between bamboo fibers, and fibers in the compression region of the specimen were crushed and bulged outward. Similar to failure mode I, failure mode II was caused by an imbalance of deformation between the compression zone and the non-compression zone. According to Figure 4 (c, d), the transverse crack on the specimen was usually located on the same horizontal line as the lower end of the semicircular hole. In the TR group, failure mode II was predominant. When the thickness of the specimen was large, the cracks were discontinuous and the deformation in the specimen's center was not evident (Fig. 4 (c)); however, when the specimen thickness was small, the opposite phenomenon was observed (Fig. 4 (d)).

3.1.5 Failure mode III

The Mode III failure was a splitting failure between bamboo fibers, and it only occurred in the RL group of specimens. Because bamboo's fundamental structure is easily deformed, the stress was primarily concentrated at the bottom of the half-hole. In the center of the specimen, a long, vertical crack appeared, with smaller cracks surrounding the semicircular hole. As the bolt was gradually inserted into the specimen, numerous small cracks appeared in the area of compression. As the load increased, the cracks in the center of the specimen gradually widened in the loading direction, resulting in the eventual failure of the specimen (Fig. 4 (e)).3.1.6 Failure mode IV

Failure mode IV was the shear failure of the adhesive layer, and all specimens of group TL exhibited this mode. At the beginning of the load process, there was no visible damage to the specimen; however, once the maximum load was reached, a large vertical crack appeared, and the load dropped. Among all failure modes, the mode IV specimen had the smallest ultimate load, which was less than 3 mm, as shown in Fig. 4 (f).

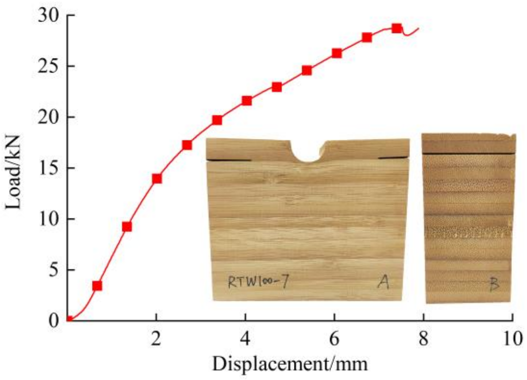

(a) Failure mode I—small diameter and large width

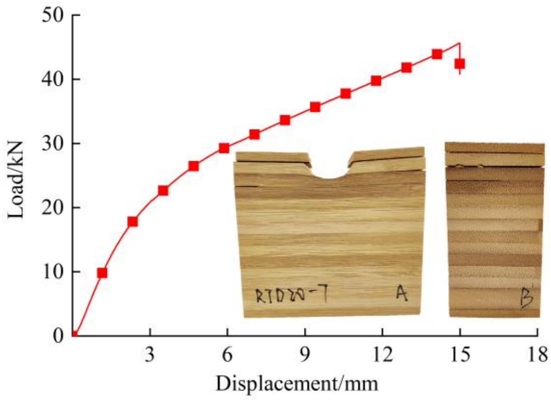

(b) Failure mode I—large diameter and small width

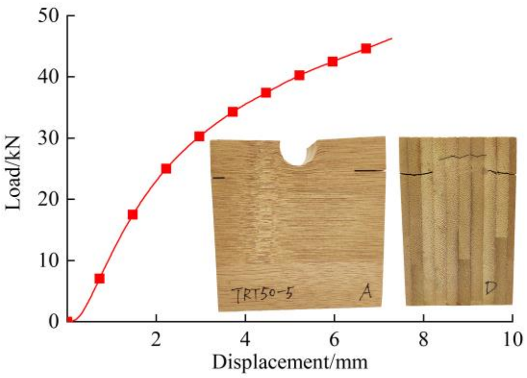

(c) Failure mode II—large thickness

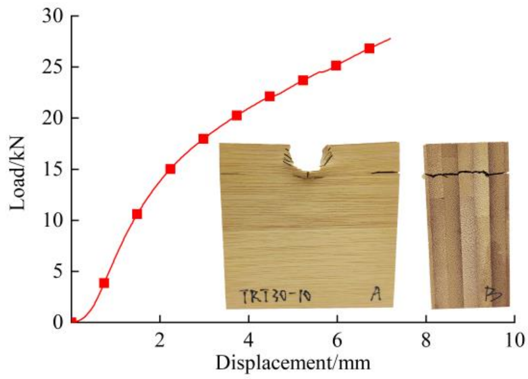

(d) Failure mode II—small thickness

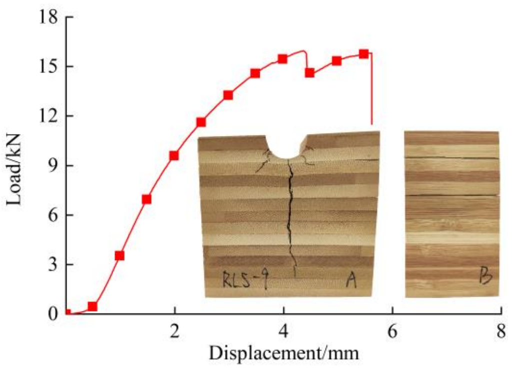

(e) Failure mode III

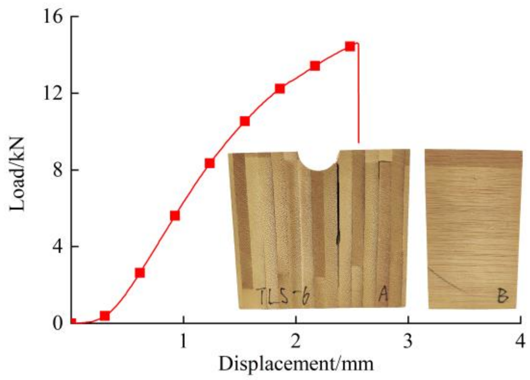

(f) Failure mode IV

Fig. 4. Four failure modes and the load-displacement curves of typical specimens

3.2 Effect of multiple variables on the dowel-bearing strength of LFBL

3.2.1 Arrangement method of flattened-bamboo panels

As illustrated in Fig. 5, the load-displacement curves of specimens with different arrangements of flattened bamboo panels varied significantly. Among the TR group of specimens, the dowel-bearing capacity was the greatest, followed by the RT group, which had the greatest ultimate displacement. Dowel-bearing capacity of the RL and TL groups of specimens was significantly lower than that of the other two groups, and the TL group's ultimate displacement was the smallest, indicating brittleness. Combined with the failure phenomenon described in Section 3.1, it is not difficult to conclude that high shear stresses in the weaker adhesive layer can result in rapid fracture and low strength in TR specimens.

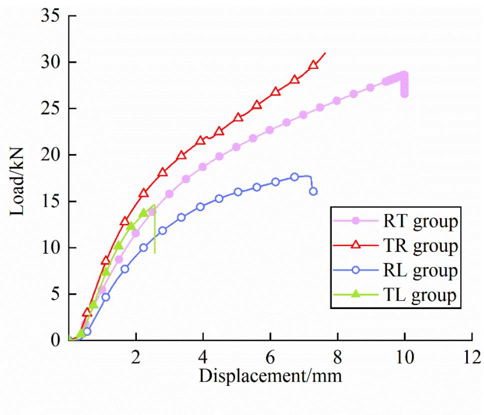

(a) The average load-displacement curves

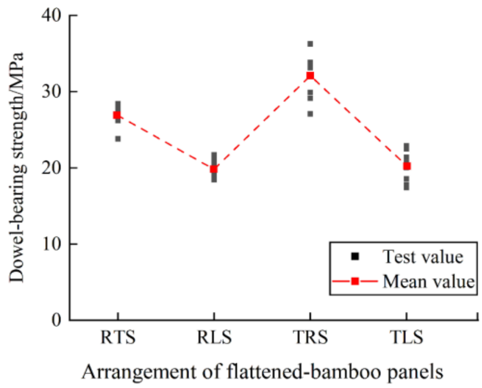

(b) The dowel-bearing strength

Fig. 5. Comparison of different arrangement method of flattened-bamboo

3.2.2 The diameter of bolts

When the diameters of the bolts were 16 mm, 18 mm, and 20 mm, group RT specimens could achieve the ultimate load. For all other specimens in groups RT and TR, the bolt was already embedded in the specimen before the material was fully compressed, causing the test to be terminated, resulting in the absence of a falling section in their load-displacement curves (see Fig. 6 (a, c).)

As shown in Fig. 6 (b, d), the effect of bolt diameter on dowel-bearing capacity was consistent: the calculated 5% *D* off-set dowel-bearing strength tended to decrease as bolt diameter increased.

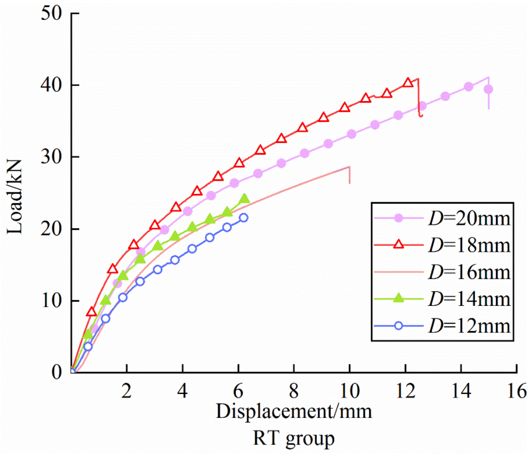

(a) The average load-displacement curves of RT group

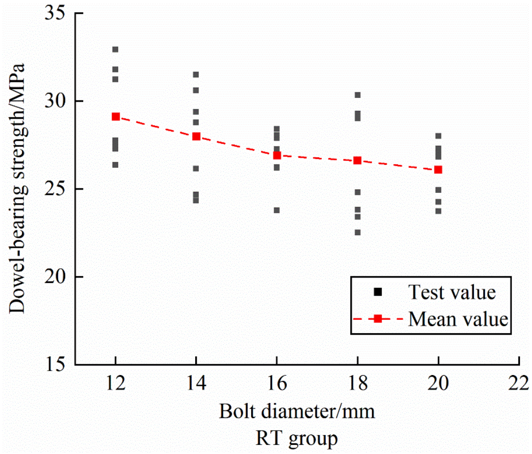

(b) The dowel-bearing strength of RT group

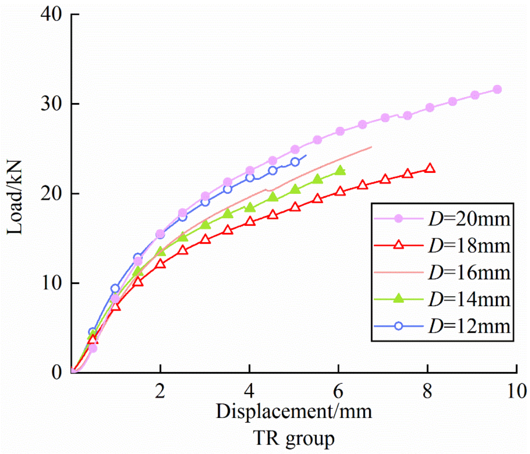

(c) The average load-displacement curves of TR group

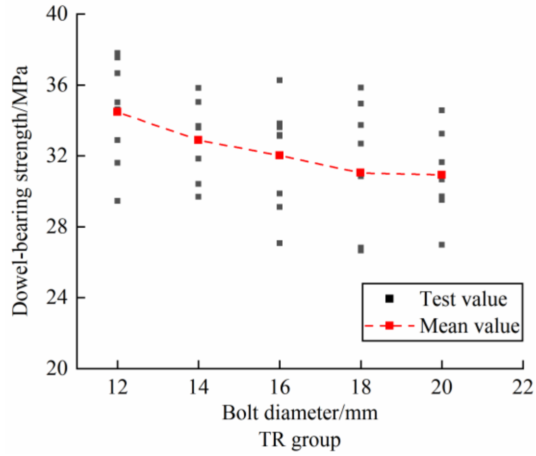

(d) The dowel-bearing strength of TR group

Fig. 6. Comparison of different diameter of bolts

3.2.3 Dimensions of specimen

(1) Effect of length

As depicted in Fig. 7 (a-d), the average 5% *D* dowel-bearing strength of groups RT and TR was 26.7 MPa, while that of group RT was 32.4 MPa, indicating that the dowel-bearing strength did not change as specimen length increased, as long as the minimum length requirement was meeting.

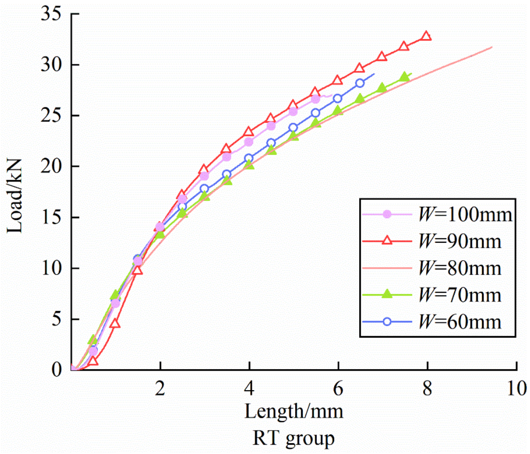

(a) The average load-displacement curves of RT group

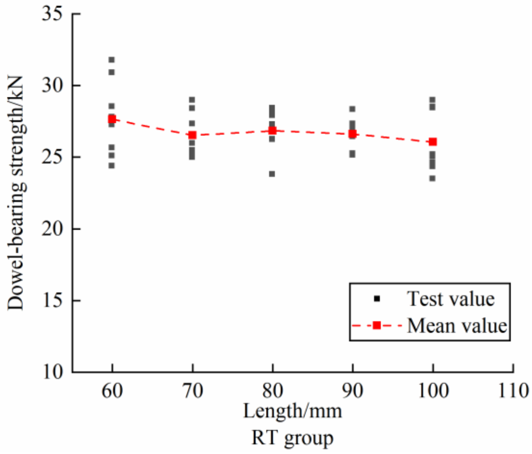

(b) The dowel-bearing strength of RT group

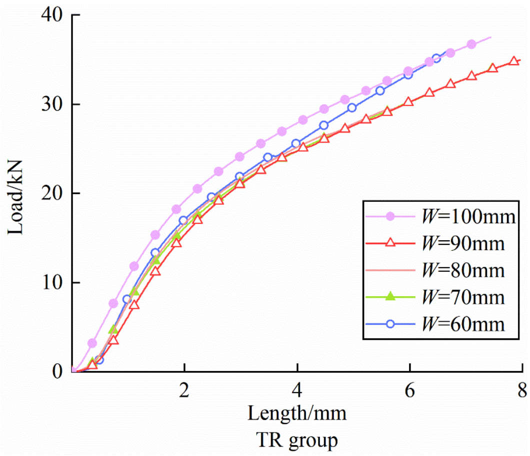

(c) The average load-displacement curves of TR group

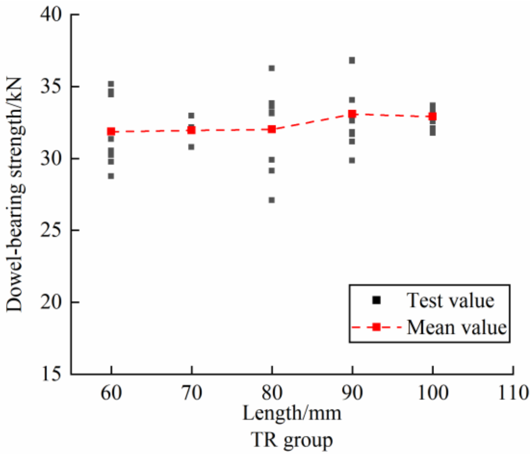

(d) The dowel-bearing strength of TR group

Fig. 7. Comparison of different length of specimens

(2) Effect of width

With an increase in specimen width, the ultimate load and dowel-bearing strength of RT group specimens increased. As previously stated, the wider the width, the less noticeable the cracks. Nonetheless, when the width exceeded 80 mm, the dowel-bearing strength was nearly constant at 27 MPa (Fig. 8 (a, b)).

The dowel-bearing strength of TR group specimens fluctuated slightly as the width increased from 60 mm to 100 mm, but there was no discernible trend. In this regard, it may be considered that the width had no effect on the strength of specimens in the TR group, which averaged 33 MPa (Fig. 8 (c, d)).

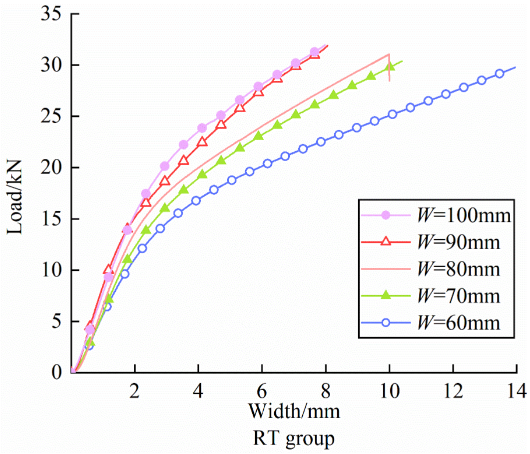

(a) The average load-displacement curves of RT group

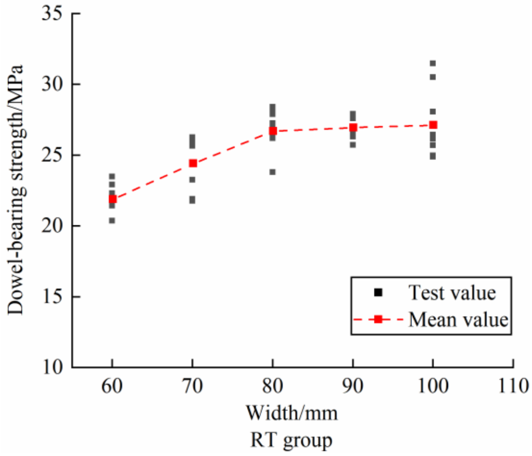

(b) The dowel-bearing strength of RT group

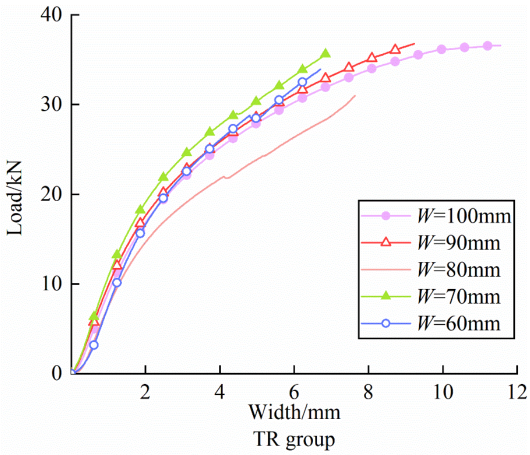

(c) The average load-displacement curves of TR group

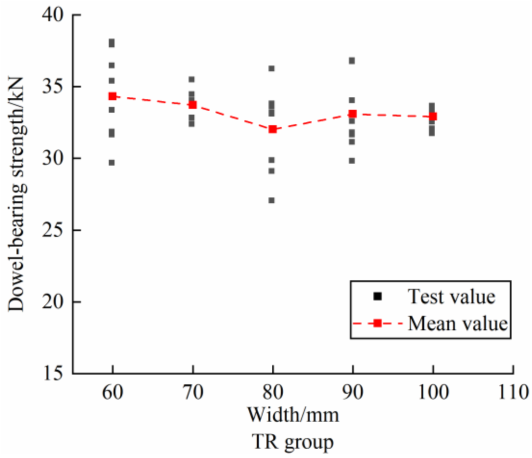

(d) The dowel-bearing strength of TR group

Fig. 8. Comparison of different width of specimens

(3) Effect of thickness

For RT group specimens, the 5% *D* dowel-bearing strength of specimens with different thicknesses clustered around 25 MPa with a small fluctuation degree and no clear trend in the variation between the mean values, indicating that thickness had no effect on the strength of RT specimens (Fig. 9 (a, b)).

The TR specimen's load displacement curve (Fig. 9 (c)) revealed the following phenomenon: The load at a low thickness level was significantly lower than at a high thickness level. Due to local cracking, when the thickness of the specimen was large, a crack developed slowly on the bonding surface and did not rapidly evolve into a complete failure. The 5% D dowel-bearing strength increased as the thickness increased, which was consistent with the trend of bearing capacity, as shown in Fig 9 (d).

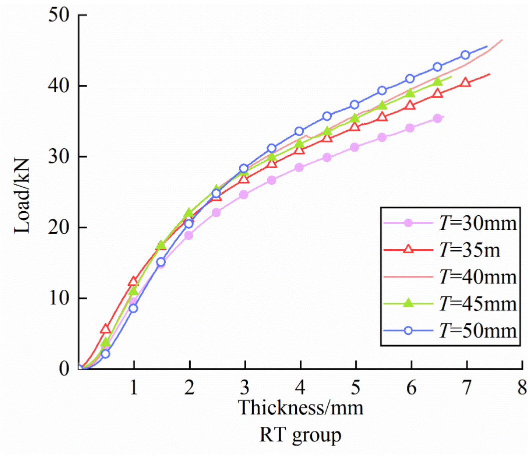

(a) The average load-displacement curves of RT group

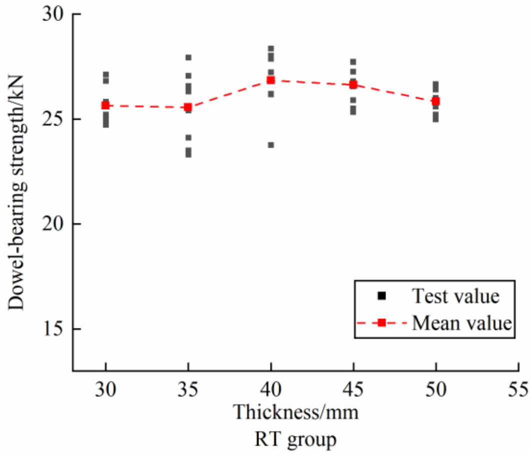

(b) The dowel-bearing strength of RT group

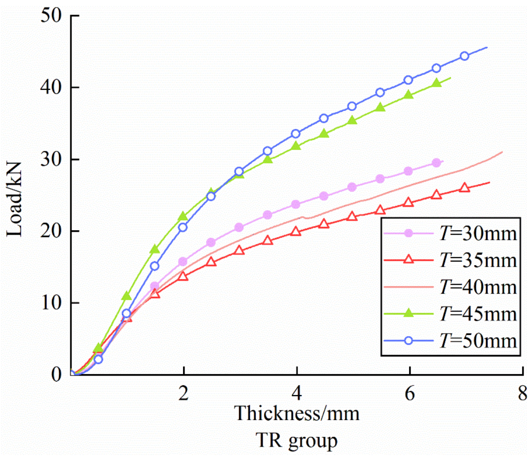

(c) The average load-displacement curves of TR group

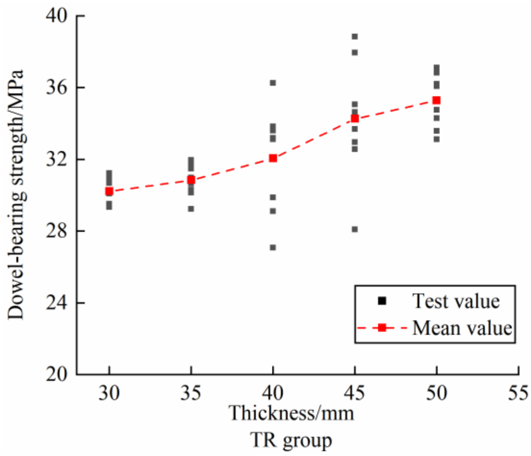

(d) The dowel-bearing strength of TR group

Fig. 9. Comparison of different thickness of specimens

In conclusion, the dimensions had varying effects on the dowel-bearing strength of specimens based on the bamboo panel arrangement method. In the half-hole test of the dowel-bearing strength of LFBL, the recommended specimen dimensions were $L \geqslant 5D$, $W \geqslant 5D$, and $T \geqslant 3D$ based on the above results.

3.4 Comparison between LFBL and other bamboo-or-wood products

This paper compared the dowel-bearing strength of RT and TR specimens with other bamboo-or-wood products, such as larch laminated wood (LLW) [33], glulam bamboo

(GB) [34], tropical hard woods (THW) [35], and glued laminated Guadua bamboo (GLGB) [36]. T There was a low coefficient of variation of less than 15% in the density of selected materials, ranging from 0.5 to 1.5 grams per cubic centimeter. Fig. 10 illustrates a rough division of the diameter of the bolt into four levels: 12 mm, 16 mm, 18 mm, and 20 mm. When the bolt diameters varied, the dowel-bearing strength of LFBL was comparable to bamboo or wood products, and at some diameter levels, it was even superior. In conclusion, LFBL is capable of replacing engineered wood due to its mechanical properties. This conclusion is also supported by the test results of other materials, which indicate that, under the same conditions, the TR group specimens exhibited a greater dowel-bearing strength than the RT group specimens, which is consistent with the conclusion reached in this paper.

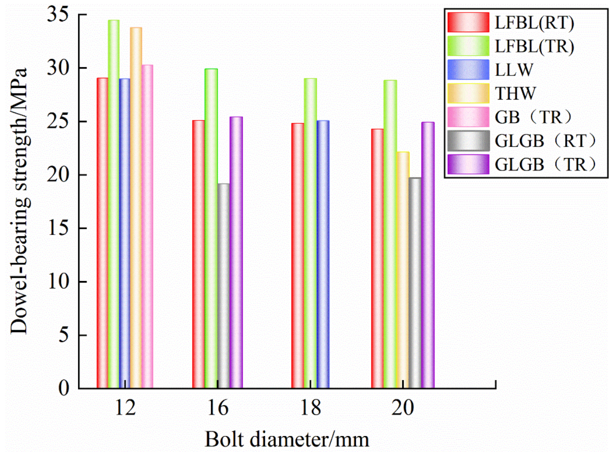

Fig. 10. Comparison between LFBL and other bamboo-or-wood products

3.5 Calculation

For the dowel-bearing strength of wood products, there are many calculation methods in different national standards and publications, which mainly based on the compressive strength or considering the influence of density and bolt diameter. This paper compared the calculation results from various methods for RT and TR specimens, and the applicability of different calculation formulas to the prediction of dowel-bearing strength of LFBL perpendicular to grain was evaluated.

3.5.1 Eurocode 5 [37]

The Eurocode 5 is based on the bolt diameter and material density. There are also differences between different materials:

$$f_{\mathrm{e,y}} = 0.082(1-0.01D)\rho_{\mathrm{k}}/K_{90}$$
$$K_{90} = \begin{cases} 1.35+0.015D & \text{Softwood} \\ 0.90+0.015D & \text{Hardwood} \end{cases} \tag{2}$$

Where, $f_{\mathrm{e,y}}$ is the 5%D off-set dowel-bearing strength/MPa, D is the bolt diameter/mm, ρ_{k} is the density of timber/kg/m^3.

3.5.2 NDS [38]

NDS is also based on material density and bolt diameter:

$$f_{\mathrm{e,y}} = 212G^{1.45}D^{-0.5} \tag{3}$$

Where, G is the density of timber/g/cm^3.

3.5.3 CSA [39]

The theoretical calculation equation of the dowel-bearing strength of timber perpendicular to grain in Canadian Standard Association is shown in Eq. (4):

$$f_{\mathrm{e,y}} = 22G(1-0.01D) \tag{4}$$

3.5.4 GB 50005 [40]

In Chinese GB 50005, The dowel-bearing strength mainly depends on the design value of compressive strength of wood:

$$f_{\mathrm{e,y}} = K_{90} f_{\mathrm{c}} \tag{5}$$

Where, f_{c} is the design value of compressive strength of wood/MPa; K_{90} is the adjustment coefficient, as in Table 4 [40].

Table 4 [40] The adjustment coefficient of the dowel-bearing strength of wood perpendicular to grain

D/mm	8	10	12	14	16	18	20	22	24
Adjustment coefficient	0.85	0.75	0.68	0.65	0.60	0.56	0.54	0.51	0.50

3.5.5 Ramirez et al. [36]

Fernando et al. proposed Eq. (6) for calculating the dowel-bearing strength of laminated Guadua bamboo perpendicular to grain based on bolt diameter:

$$f_{\mathrm{e,y}} = 89.9D^{-0.38} \tag{6}$$

3.5.6 Li [11]

Li studied the dowel-bearing strength of PBSL parallel and perpendicular to grain, and proposed Eq. (7) based on the bolt diameter and the compressive strength:

$$f_{\mathrm{e,y}} = \left[3.673(D/10)^2 - 10.59(D/10) + 10.15\right] f_{\mathrm{c,90}} \tag{7}$$

Where, $f_{\mathrm{c,90}}$ is the compressive strength of PBSL perpendicular to grain/MPa.

The above equations are all related to the bolt diameter, therefore, the applicability of the above equations is verified by the specimens with different bolt diameters in this paper. As can be seen from Table 6, the calculated dowel-bearing strength by Li's equation was too high, while by CSA was too conservative, indicating that the method of high-density materials is not applicable to low-density materials when calculating the dowel-bearing strength. Fig. 11 shows the comparison between other theoretical calculated values and the test values.

For specimens of TR group, the predicted 5%*D* dowel-bearing strength of Eurocode 5 and Eq. (6) were almost in good agreement with the test values, which can be used to predict the dowel-bearing strength of LFBL perpendicular to grain. The equation recommended by GB50005 to calculate the perpendicular-to-grain dowel-bearing strength is based on the parallel-to-grain compressive strength of wood, and bamboo is more anisotropic than wood, resulting the values obtained by this method deviated from the test values. The method of NDS is also not appropriate for LFBL as the predicted value of it was largest among these methods. For specimens of RT group, the tested dowel-bearing strength was too little compared with that obtained from all equations.

To sum up, it is necessary to put forward new equations suitable for predicting the dowel-bearing strength of LFBL perpendicular to grain.

Table 5 Comparison of dowel-bearing strength values calculated by different equations

D/mm	$f_{e,y}$/MPa							
	Test values		The calculation results of different equations					
	RT	TR	Eurocode 5	NDS	CSA	GB 50005	Ramirez	Li
12	29.0	34.6	35.0	39.8	14.4	38.2	35.0	51.9
14	27.9	32.9	33.6	36.8	14.1	36.5	33.0	47.9
16	26.8	32.0	32.2	34.5	13.7	33.7	31.4	49.6
18	26.5	28.1	30.8	32.5	13.4	31.5	30.0	56.8
20	26.0	28.2	29.5	30.8	13.1	30.4	28.8	69.6

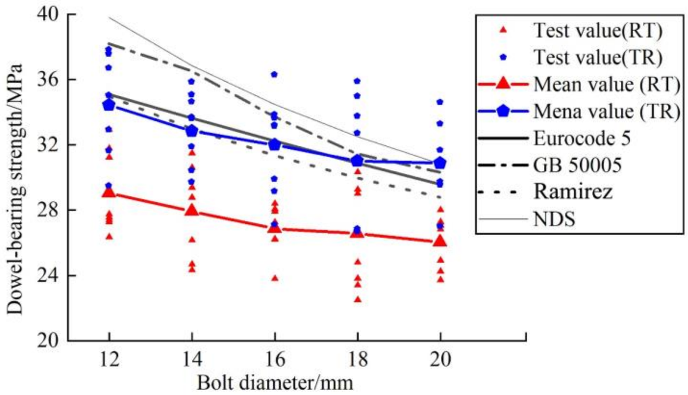

Fig. 11. The comparison between the prediction results of different method and the test values

3.6 Equations for dowel-bearing strength of LFBL perpendicular to grain

3.6.1 Specimens of RT group

When the dimensions of the specimens were satisfied with the size recommended in this paper, the dowel-bearing strength of the RT group of specimens was no longer affected by the size. Therefore, for RT group, an empirical equation was proposed in this paper adopted the model similar to Li[11] and Cui et al.[31], where the concept of material compressive strength was introduced, and the design was based on bolt diameter without considering size effect. The theoretical formula is expressed as:

$$f_{e,R} = K_D f_c \tag{8}$$

Where, $f_{e,R}$ is the dowel-bearing strength of RT group of specimens/MPa, K_D is the influence coefficient of bolt diameter, $f_{c,R}$ is the compressive strength of RT specimens/MPa.

With D as abscissa and f_e/f_c as ordinate, K_D was obtained by regression fitting on quadratic polynomial, and there is a high degree of coincidence as R^2=0.982 (Fig. 12 (a)). By substituting the influence coefficient into Eq. (8), the empirical equation for calculating the dowel-bearing strength of LFBL-RT specimens can be expressed as:

$$f_{e,R} = \left[0.0008(D)^2 - 0.034D + 0.97\right] f_{c,R} \tag{9}$$

3.6.2 Specimens of TR group

In the existing studies, scholars have not reached a unanimous conclusion on the influence of size on the dowel-bearing strength, but the test results showed that the dowel-bearing strength of TR specimen was affected by the bolt diameter and the thickness of the specimen. Therefore, an empirical formula was proposed according to the compressive strength of LFBL perpendicular to grain, bolt diameter, and the thickness, can be expressed as:

$$f_{e,T} = K f_{c,T} \tag{10}$$

Where, $f_{e,T}$ is the dowel-bearing strength of TR group of specimens/MPa, K is the influence coefficient of bolt diameter and thickness, $f_{c,T}$ is the compressive strength of TR specimens/MPa.

Variance analysis was conducted on the test values of TR specimens, and the results were shown in Table 6. It was found that the Sig. Value of bolt diameter was 0.04 greater than that of specimen thickness, which was 0, indicating that the thickness of specimens had a greater influence on the dowel-bearing strength (Sig. Value represents the significance of the influence of the indicator on the dependent variable, and the smaller the value is, the more significant the influence is). Meanwhile, the variation trend of dowel-bearing strength is opposite with the increase of this two. Therefore, with the $T/\sqrt{D}$ as abscissa and f_e/f_c as ordinate, quadratic polynomial was used for regression fitting, and the value of R^2 is 0.970. Combining the influence coefficient with Eq. (10), the empirical equation for dowel-bearing strength of LFBL-TR specimens can be obtained as:

$$f_{e,T} = \left[-0.006\left(T/\sqrt{D}\right)^2 - 0.066\left(T/\sqrt{D}\right) + 1.716\right] f_{c,T} \tag{11}$$

Table 6 Variance analysis for dowel-bearing bearing strength of TR specimens

Influence factors	Sum of squares	Degree of freedom	Mean square	*F*	Sig.
Corrected model	221[a]	8	27.7	4.3	0
Intercept	12606	1	12606	1968	0
D	152	4	38.1	5.9	0
T	68.9	4	17.2	2.7	0.04
Error	403	63	6.4		
total	76264	72			
Corrected error	624	71			

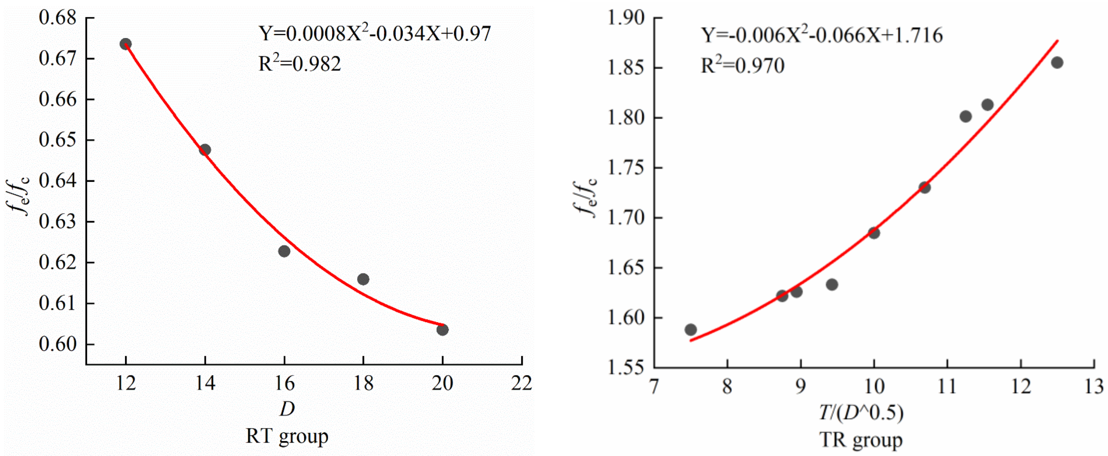

(a) The regression equation of RT specimens (b) The regression equation of TR specimens

Fig. 12. The regression equation of specimens of LFBL perpendicular to grain

4 Conclusions

In this paper, the dowel-bearing strength of LFBL perpendicular to grain was studied according to ASTM D5764, through the analysis of the test results, the following conclusions are drawn:

(1) The 5% D off-set dowel-bearing strength of LFBL perpendicular to grain in RT group was 26.3 MPa with COV=8.7%, in TR was 32.6 MPa with COV=8.1%, in RL group was 19.8 MPa with COV=6.4%, and in TL group was 20.2 MPa with COV=10.4%. Four typical failure modes were proposed: peeling failure of the adhesive layer, tearing failure between bamboo fibers, splitting failure, and brittle failure of adhesive layer. The dowel-bearing strength of RT and TR groups was comparable to that of other bamboo and wood products.

(2) The influence of various factors on the dowel-bearing strength of LFBL was studied. The specimen length had no effect on the dowel-bearing strength for both TR and RT specimens. The dowel-bearing strength of TR group was not affected by specimen width, while it of RT group would increase and gradually stabilize as the width increased. For specimens of TR group, the increase in specimen thickness contributed to the improvement of the dowel-bearing strength, while for specimens of TR group, the calculated dowel-bearing strength nearly remained constantly. However, increasing the bolt diameter would decrease the dowel-bearing strength of both RT and TR specimens. Based on test results, the recommended dimensions of specimens tested by half-hole method were $L \geqslant 5D$, $W \geqslant 5D$, $T \geqslant 3D$.

(3) By comparing the test results and the predictions of dowel-bearing strength calculated by different formulas, two empirical equations with higher accuracy were proposed for calculating the dowel-bearing strength of LFBL test samples.

Funding

This work was supported by the National Natural Science Foundation of China (No. 51878354 & 51308301), the Natural Science Foundation of Jiangsu Province (No. BK20181402 & BK20130978), 333 talent high-level projects of Jiang-su Province, and Qinglan Project Fund of Jiangsu Higher Education Institutions.

CRediT authorship contribution statement

Haitao Li: Conceptualization, Funding acquisition, Supervision, Investigation, Formal analysis, Writing - original draft. **Yue Chen:** Investigation, Formal analysis, Writing - original draft. **Dong Yang:** Supervision, Investigation,Writing - review & editing. **Rodolfo Lorenzo:** Supervision, Writing - review & editing. **CongGan Yuan:** Supervision, Investigation.

Declaration of competing interest

The authors declare that they have no known competing financial interests or personal relationships that could have appeared to influence the work reported in this paper.

Acknowledgments

The writers gratefully acknowledge Wei Xu, Chen Chen, Bingyu Jan, Tingting Ling, Gensheng Chen, Wenjing Zhou and others from the Nanjing Forestry University for helping with the tests.

References

[1] Zhou K, Li HT, Dauletbek A, Dong Y, Xiong ZH, Lorenzo R, Zhou K, Corbi I, Corbi O. Slenderness ratio effect on the eccentric compression performance of chamfered laminated bamboo lumber columns. Journal of Renewable Materials, 2022, 10(1): 165–182. https://doi.org/10.32604/jrm.2021.017223

[2] Wei Y, Zhou MQ, Chen DJ. Flexural behavior of glulam bamboo beams reinforced with near surface mounted steel bars. Materials Research Innovations, 2015, 19(s1): 98-103. https://doi.org/10.1179/1432891715Z.0000000001377

[3] Li HT, Chen B, Fei BH, Li H, Xiong ZH, Lorenzo R, Fang CH, Ashraf M. Mechanical properties of aramid fiber reinforced polymer confined laminated bamboo lumber column under cyclic loading. European Journal of Wood and Wood Products, 2022. https://doi.org/10.1007/s00107-022-01816-4

[4] Zhou YH, Huang YJ, Sayed U, Wang Z. Research on dynamic characteristics test of wooden floor structure for gymnasium. Sustainable Structures, 2021, 1(1): 000005. https://doi.org/10.54113/j.sust.2021.000005

[5] Tu DY, Chen CF, Zhou QF, et al. Research progress of thermo-mechanical compression techniques for wood products[J]. Journal of Forestry Engineering, 2021, 6(1): 13-20. https://doi.org/10.13360/j.issn.2096-1359.202001036 .

[6] Leng WQ, He S, Zhang XF, et al. Research progress and thoughts on the modification mechanism of wood furfurylation. Journal of Forestry Engineering, 2021, 6(6): 35-43. https://doi.org/10.13360/j.issn.2096-1359.202012001

[7] Ponzo FC, Antonio DC, Nicla L, Nigro D. Experimental estimation of energy dissipated by multistorey post-tensioned timber framed buildings with anti-seismic dissipative devices. Sustainable Structures, 2021, 1(2): 000007. https://doi.org/10.54113/j.sust.2021.000007.

[8] Yong C, Guan MJ, Zhang QS. Selected physical and mechanical properties of bamboo and poplar composite OSB with different hybrid ratios. Key Engineering Materials. Trans Tech Publications Ltd, 2012, 517: 87-95. https://doi.org/10.4028/www.scientific.net/KEM.517.87

[9] Su JW, Li HT, Xiong ZH, Lorenzo R. Structural design and construction of an office building with laminated bamboo lumber. Sustainable Structures, 2021, 1(2): 000010. https://doi.org/10.54113/j.sust.2021.000010

[10] Escamilla EZ, Habert G. Environmental impacts of bamboo-based construction materials representing global production diversity. Journal of Cleaner Production, 2014, 69: 117-127. https://doi.org/10.1016/j.jclepro.2014.01.067

[11] Li XZ. Research on bearing performance of bolt joint for recombinant bamboo. Chinese Academy of Forestry, Beijing, China, 2013. https://doi.org/10.7666/d.Y2405233

[12] Ashraf M, Hasan MJ, Al-Deen S. Semi-rigid behavior of stainless steel beam-to-column bolted connections. Sustainable Structures, 2021, 1(1): 000002. https://doi.org/10.54113/j.sust.2021.000002.

[13] Wang SX, Li HT, Cheng GS, Xiong ZH, Ashraf M. Mechanical behaviors of bolted steel laminated bamboo lumber connections loaded perpendicular to grain. Construction and Building Materials, 2022, 345: 128302. https://doi.org/10.1016/j.conbuildmat.2022.128302

[14] Quenneville JHP, Mohammad M. On the failure modes and strength of steel-wood-steel bolted timber connections loaded parallel-to-grain. Canadian journal of civil engineering, 2000, 27(4): 761-773. https://doi.org/10.1139/cjce-27-4-761

[15] Mahdavi M, Clouston PL, Arwade SR. Development of laminated bamboo lumber: review of processing, performance, and economical considerations. Journal of Materials in Civil Engineering, 2011, 23(7): 1036-1042. https://doi.org/10.1061/(ASCE)MT.1943-5533.0000253

[16] Dauletbek A, Li HT, Xiong ZH, Lorenzo R. A review of mechanical behavior of structural laminated bamboo lumber. Sustainable Structures, 2021, 1(1): 000004. https://doi.org/10.54113/j.sust.2021.000004.

[17] Lou ZC, Wang QY, Sun W, Zhao YH, Wang XZ, Liu XR, Li YJ. Bamboo flattening technique: A literature and patent review. European Journal of Wood and Wood Products, 2021, 79(5): 1035-1048. https://doi.org/10.1007/s00107-021-01722-1

[18] Zhang QS. Research on bamboo Research on glued bamboo panel—I. Softening and flattening of bamboo. Journal of Nanjing Forestry University (Natural Science Edition), 1988(4): 13-20. https://doi.org/10.3969/j.jssn.1000-2006.1988.04.002

[19] Li T, Cheng D, Wålinder MEP, Zhou D. Wettability of oil heat-treated bamboo and

bonding strength of laminated bamboo board. Industrial Crops and Products, 2015, 69: 15-20. https://doi.org/10.1016/j.indcrop.2015.02.008

[20] Fang CH, Jiang ZH, Sun ZJ, et al. An overview on bamboo culm flattening. Construction and Building Materials, 2018, 171: 65-74. https://doi.org/10.1016/j.conbuildmat.2018.03.085

[21] Li YJ, Lou ZC. Progress of bamboo flatten technology research[J]. Journal of Forestry Engineering, 2021(in Chinese). https://doi.org/10.13360/j.issn.2096-1359.202012021

[22] American Society for Testing and Materials, Standard test method for evaluating dowel-bearing strength of wood and wood-based products, 2013. ASTM D5764-97a.

[23] British Standards Institution, BS EN 383: Timber Structures. Test Methods. Determination of Embedding Strength and Foundation Values for Dowel Type Fasteners, BSI, London, 2007.

[24] Santos CL, De Jesus AMP, Morais JJL, Lousada J. A Comparison between the EN 383 and ASTM D5764 Test Methods for Dowel-Bearing Strength Assessment of Wood: Experimental and Numerical Investigations. Strain, 2010, 46(2): 159-174. https://doi.org/10.1111/j.1475-1305.2008.00570.x

[25] Khoshbakht N, Clouston PL, Arwade SR, Schreyer AC. Evaluation of ASTM d5764 dowel connection tests for laminated veneer bamboo (LVB). Journal of Testing and Evaluation, 2019, 47(4): 20180385. https://doi.org/10.1520/JTE20180385

[26] Ottenhaus LM, Li Z, Crews K. Half hole and full hole dowel embedment Strength: A review of international developments and recommendations for Australian softwoods. Construction and Building Materials, 2022, 344: 128130. https://doi.org/10.1016/j.conbuildmat.2022.128130

[27] Cui ZY, Xu M, Tu LH , Chen ZF, Hui B. Determination of dowel-bearing strength of laminated bamboo at elevated temperatures. Journal of Building Engineering, 2020,

30: 101258. https://doi.org/10.1016/j.jobe.2020.101258

[28] Rammer DR. Parallel-to-grain dowel-bearing strength of two Guatemalan hardwoods. Forest products journal, 1999, 49: 77-87. https://doi.org/10.1023/A:1009223516957

[29] Sawata K, Yasumura M. Determination of embedding strength of wood for dowel-type fasteners. Journal of Wood Science, 2002, 48(2): 138-146. https://doi.org/10.1007/BF00767291

[30] Whale LRJ, Smith I. The derivation of design classes for nailed and bolted joints in Eurocode 5. International Council for Building Research Studies and Documentation, Working Commission W18–Timber Structures, 1988.

[31] Cui ZY, Tu LH, Xu M, Chen ZF, Wang CX. The evaluation of dowel-bearing properties of laminated bamboo parallel to grain. Structures. Elsevier, 2020, 25: 956-964. https://doi.org/10.1016/j.istruc.2020.04.004

[32] ASTM International. Standard test methods for small clear specimens of timber ASTM D143-2014. US, ASTM International, 2014.

[33] Liu KZ. Connection Design and Bearing Performance Evaluati on for Larch Laminated Wood Beams and Columns. Beijing：Chinese Academy of Forestry, 2011. https://doi.org/10.7666/d.D603301

[34] Eratodi IGLB, Triwiyono A, Awaludin A, Prayitno TA. The effect of specific gravity on embedding strength of glued laminated (glulam) bamboo: Numerical analysis and experiment. ASEAN Engineering Journal, 2014, 3(1): 30-40. https://doi.org/10.11113/aej.v3.15394

[35] Hassan R, Ibrahim A, Ahmad Z, Yusoff M. Dowel-bearing strength properties of two tropical hardwoods. InCIEC 2013. Springer, Singapore, 2014: 27-36. https://doi.org/10.1007/978-981-4585-02-6_3

[36] Ramirez F, Correal JF, Yamin LE, Atoche JC. Dowel-bearing strength behavior of glued laminated Guadua bamboo. Journal of Materials in Civil Engineering, 2012, 24(11): 1378-1387. https://doi.org/10.1061/(ASCE)MT.1943-5533.0000515

[37] The European Standard EN 1995-1-1: 2014(E), Eurocode 5: Design of Timber Structures-Part 1-1: General-common rules and rules for buildings; 2014.

[38] American Forest & Paper Association, ANSI/AF&PA NDS-2015 National Design Specification for Wood Construction. AF&PA, Washington, D.C., 2015.

[39] Canadian Standard Association (CSA). Engineering design in wood. Mississauga, Ontario, Canada, 2009.

[40] Ministry of Construction, PRC. GB 50005-2017. Standard for design of timber structures. 2017.